Int. J. Therm. Sci. (1999) 38, 424–435

Comparison of experimental values and numerical simulation on a set-up simulating the cross-section of a disc-type transformer

Jean-Michel Mufuta M. B.

Department of Mechanical Engineering, KU Leuven, Celestijnenlaan 300 A, B-3001 Heverlee, Belgium

(Received 21 April 1998, accepted 29 September 1998)

Abstract — A model simulating a part of the cross-section of a transformer has been designed to validate numerical simulations. The model is composed of a transformer box ($0.48 \times 0.66 \times 0.2$) connected to a cooler. The transformer box is composed of two columns of 6 heating blocks ($0.07 \times 0.14 \times 0.2$) in-line arranged. Some thermocouples are placed inside the blocks and some others in the fluid to measure temperature field. The velocity field is measured by means of LDV technique. For that reason, the frontal wall of the transformer box is in Plexiglas. The resolution of the laser doppler velocimeter (LDV) is 0.1609, 0.1605, and 2.2233 (mm) in respectively the x, y and z directions. Experiments were performed in a flow rate range: 0.1, ..., 0.3 $m^3 \cdot h^{-1}$ using water as the cooling medium. This yields a mixed convection laminar regime for the whole range. Numerical calculations using a finite difference technique were simulated with boundary conditions matching those of the experiments. Some adjustments for grid refinement as well as those of the numerical parameters were required to cover uncertainties due to assumptions and simplifications (idealisations) and to get good agreements with results. The computer code used is PHOENICS. © Elsevier, Paris.

experiments/ velocity and temperature measurements/ laser doppler velocimeter / numerical calculations

Résumé — Comparaison entre les valeurs expérimentales et de calcul numérique pour l'écoulement dans un banc d'essais simulant la coupe longitudinale d'un transformateur de type disque. Un modèle simulant une partie de la section longitudinale d'un transformateur de puissance de type disque a été conçu dans le but de valider le calcul numérique. Ce modèle est composé d'un boîtier ($0{,}48 \times 0{,}66 \times 0{,}2$) relié à un refroidisseur. À l'intérieur du boitier, deux colonnes de 6 blocs chauffants ($0{,}07 \times 0{,}14 \times 0{,}2$) alignés y sont placées. Afin de mesurer le champ de température, des thermocouples sont placés aussi bien dans les blocs que dans le fluide. Le champ de vitesse est quant à lui mesuré par la technique du laser (LDV). Pour ce faire, la face frontale du boîtier est en plexiglas. La résolution du laser utilisé est de $0{,}1609 \times 0{,}1605 \times 2{,}2233$ [mm] dans les directions x, y et z, respectivement. Les différents essais ont été effectués avec des débits d'eau situés dans la gamme 0,1 ..., 0,3 $m^3 \cdot h^{-1}$, entraînant un régime de convection laminaire mixte pour toute la gamme. Des simulations numériques basées sur les différences finies ont été effectuées avec des conditions aux limites équivalentes à celles des essais. Quelques raffinements du maillage, ainsi que des ajustements des paramètres numériques, ont été nécessaires pour obtenir des résultats équivalents. Le logiciel de calcul utilisé pour la simulation est Phoenics. © Elsevier, Paris.

expérience / mesure des temperatures et des vitesses / vélocimétrie laser doppler / calcul numérique

Nomenclature

c_p	specific heat	$J \cdot kg^{-1} \cdot K^{-1}$
Gr	Grashof number $= \dfrac{g \beta q d^4}{k \nu^2}$	
g	gravity	$m \cdot s^{-2}$
k	thermal conductivity	$W \cdot m^{-1} \cdot K^{-1}$
K	ratio of solid to fluid thermal conductivity	
$\dot{m}$	mass flow rate	$kg \cdot s^{-1}$
n	coordinate normal to the solid–fluid interface	
Nu	Nusselt number $\dfrac{\partial T / \partial n_s \, d_h}{(T_w - T_b)}$	
Pr	Prandtl number	
Q	heat dissipation rate per block	W
R	residue	
T	temperature	°C
t	time	s

* jean-michel.mufuta@mech.kuleuven.ac.be

v	y-component of the velocity	$m \cdot s^{-1}$
$\dot{v}$	volume flow rate	$m^3 \cdot h^{-1}$
w	z-component of the velocity	$m \cdot s^{-1}$
x,y,z	Cartesian coordinates	

Greeks symbols

δ	Heaviside function	
β	expansion coefficient	K^{-1}
μ	dynamic viscosity	$kg \cdot s^{-1} \cdot m^{-1}$
ν	kinematic viscosity	$m^2 \cdot s^{-1}$
ϕ	variable value of a given iteration	

Indices

bl	block
f	cooling fluid
loss	losses
m	mean or average
w	water

1. INTRODUCTION

This manuscript compares measured and calculated values on a set-up, simulating the cross-section of a disc-type transformer. The aim of the work is to validate the numerical model by means of experimental measurements. This involves the establishment of the right settings in the code instructions: that is the grid numbers and their refinement, the under-relaxation, the good estimation of boundary conditions.

The methodology of the validation consists in comparing the temperature and velocity fields both measured and calculated and therefore in readjusting inputs to the numerical model. For this reason, numerical calculations are performed with boundary conditions matching those of the experiments. The Laser Doppler velocimeter (LDV) is used together with thermocouples to measure respectively velocity and temperature within the box. Each operation (task) i.e. numerical calculations on one hand and experiments on the other hand, is performed accurately to allow acceptable precision. Later they are compared and a new accuracy is estimated. This accuracy estimation is the percentage difference between the two types of results.

For the numerical calculations, it is to say the residues, the continuity of flux that are checked and moreover, since the simulations are monitored, it is possible to view the convergence (the rate of change of the solved for variables: temperature...). For the measured values, the RMS is used.

The final goal of this validation is to establish a reliable numerical model for further investigations of heat transfer correlations, as a function of different parameters such as the geometry, the mass flow rate, the heat dissipation rate, the fluid properties,... These correlations will not be established in this paper.

Some interesting experiments have been reported in the literature. Yamagushi et al. [1] presented a method for calculating the flow rate of circulating oil in a self-cooled transformer. The flow rate was calculated by equating the pressure loss with the thermal driving force in a circulating loop. They made some measurements on models to validate the method. LDV was used to measure the flow rate. The results agreed within 15 % of each other. Nakadate et al. [2] have developed a gas-cooling system of 275 kV, 300 MVA in order to optimise conditions for good cooling. In the model experiments gas flow was substituted by an equivalent water flow and 2-dimensional numerical flow analysis and network analysis were performed. The configuration of the transformer is that of a disc- type with directed flow (with stopper). To measure velocity distribution, tracer particles were mixed with the water and their movement was photographed using a CCD camera. The aspect ratio used was of the order 0.11,...,0.18. The numerical analysis was based on a steady-state two-dimensional symmetric flow. A finite difference method is used. Less interest has been shown for non-directed flow, as it is the case in the present work. The experimental method is presented below.

2. EXPERIMENTAL WORK

2.1 Description of the experimental set-up

The experimental set-up is shown in *figure 1*. The transformer box is described in detail in *figure 2*. The fluid flows from the bottom of the box to the top, and flows up to the top of the cooler before it reaches the pump. Thus the heat removed from the heating blocks by the fluid, by means of its motion from bottom to top, is extracted in the cooler while flowing from top to bottom. A rota flow meter is used to set the required mass flow rate. The thermocouples are all connected to a data acquisition system that allows temperature measurement at each instant in the whole field (blocks and fluid).

The velocity field is measured with a Laser Doppler velocimeter. To allow the laser beam to reach the fluid in the box, the front wall of the box is made of Plexiglas.

The heating of the blocks is performed by heating elements inserted in each block (circles in the box of *figure 2*).

The instruments used for temperature and velocity measurement were calibrated before each set of experiments.

A kilowatt hour meter is used to estimate the real quantity of electric input delivered by the power generator.

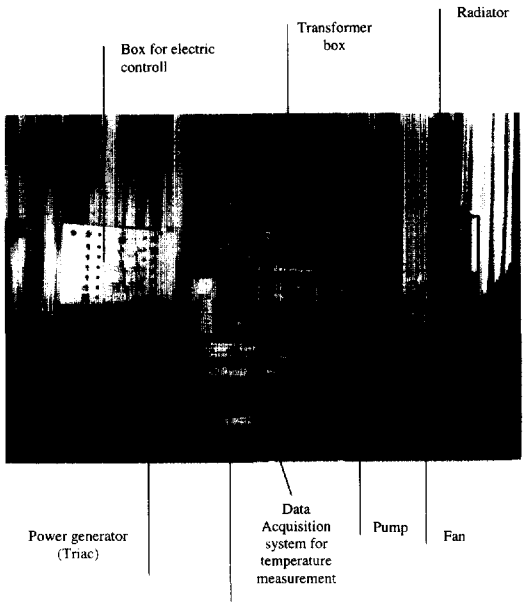

a

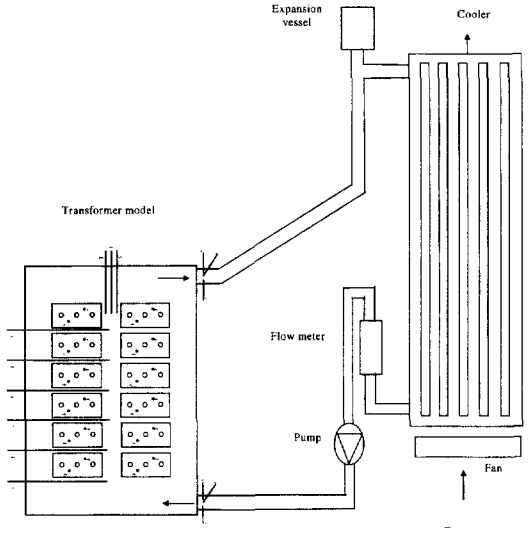

b

Figure 1. a. Experimental rig for measurements on disc type transformer model. **b.** Schematic diagram of the experimental set-up.

The energy balance method is used beside to calibrate the system. The network is presented in *figure 3.*

The inlet water from the network flowed from top (pressure relief vessel) to bottom. The mass flow rate could be fixed to a constant value, and thus measured simply by weighing a given quantity after a certain time with a high accuracy balance. The inlet water temperature was also fixed in time. Since the transformer box was completely and carefully insulated

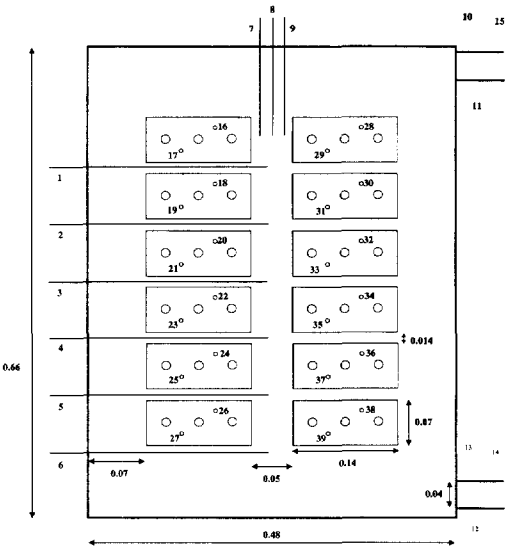

Figure 2. Schematic transformer box model (sizes are in m).

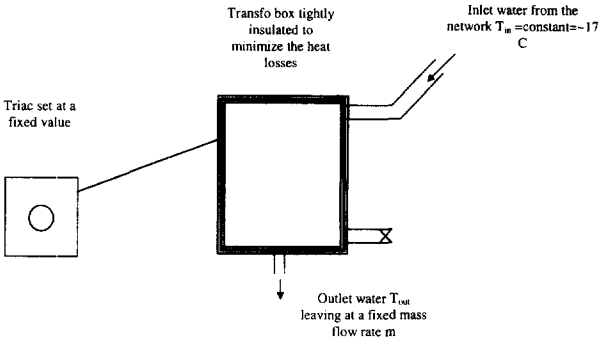

Figure 3. Network used to calibrate the Triac.

and the inside temperature field was that of the ambient temperature (which could be measured by means of thermocouples). heat losses were minimised. The heat balance can be expressed as:

$$Q_{\text{Triac}} = \dot{m}\, c_p\, (T_{\text{out}} - T_{\text{in}}) + Q_{\text{loss}} \qquad (1)$$

For T_{out} being 1 to 3 degrees above the room temperature, Q_{loss} can be neglected. Heat losses through walls for higher temperature levels have been estimated and are presented later.

The calibration of the rota flow meter used the same principle of heat balance. For this case, the fluid flows following the normal path of the set-up as described in *figure 1b.* Since for the same fixed Q_{triac} as that of the former experiment, the heat losses through the box walls being the same, the heat removed by the fluid can be matched to $\dot{m}\, c_p\, (T_{\text{out}} - T_{\text{in}})$ of equation (1). T_{out} and T_{in} are measured by thermocouples 11 and 12 on

figure 2, C_p is calculated using the average temperature of the fluid in the box. We can get thus the right value of $\dot{m}$.

Thermocouples and related reference boxes were also calibrated by measuring iced water in an insulated bottle at 0 °C. Their results were also compared with an independent reference thermocouple (not connected to the data acquisition system). They gave identical results for different measurements performed previously to the experiments.

2.2. Test performed

A set of experiments was performed to measure temperatures and velocity values in the set-up by means of the instrumentation mentioned in the preceding subsection.

Due to the horizontal orientation of the inlet and outlet, to ensure equal average velocity in the three vertical channels, the range of mass flow rates was limited to a maximum value of 0.3 $m^3 \cdot h^{-1}$. The flow pattern may thus simulate the main part of the flow in the middle of the disc stack of the transformer. For a greater value, the flow tends to pass by the first vertical channel (left vertical channel).

Table I summarises the different sets of measurement performed. In each case, the aim is to measure the temperature and velocity field. Velocity measurements were only performed for tests 2.3, 3.2, 2.2 and 1.2. Temperature values were measured in the steady state as well as in transient operation.

As mentioned in the introduction, since the aim of the present work is to validate numerical calculations for further simulations for the establishment of correlation of heat transfer in steady state, only results of steady state operation are presented here.

TABLE I
Different sets of measurement performed.

Simulation number	Test	Heat dissipation rate (W)	Mass flow rate ($m^3 \cdot h^{-1}$)
1	1.2	1 538	0.2
2	1.3	1 538	0.3
3	2.2	3 452	0.2
4	2.3	3 452	0.3
5	3.2	5 105.6	0.2
6	3.3	5 105.6	0.3
7	4.2	6 969	0.2
8	4.3	6 969	0.3

2.3. Estimation of heat losses through wall and insulation

In order to estimate the actual heat removed by the fluid, the losses through the walls of the box are estimated. This estimation is required to set real boundary conditions for numerical calculations.

Reducing the Triac and the pump, whilst monitoring the temperature evolution in the box, allowed the estimation of losses through walls. Obviously, to avoid any natural convection flow and thus uncontrolled heat transfer, gates at the outlet and the inlet of the cooler were closed. This gives an evolution of the heat content of the box considered as a whole. The following relations are used.

$$Q_l = m_{bl}\, c_{p_{bl}} \frac{\Delta T}{\Delta t} + m_w\, c_{p_w} \frac{\Delta T}{\Delta t} \qquad (2)$$

where Q_l stands for heat losses, m, C_p are mass and specific heat respectively. $\frac{\Delta T}{\Delta t}$ is the temperature difference over the time step. bl and w refer to block and water respectively.

Since no heat is removed by mass flow rate from inlet to outlet, and no heat is introduced in the system, if there is a change (decrease) of the heat content of the box, it is occurring through the walls. For the different cases, the value at the first instant of the total heat loss (the highest) is considered since, in the steady state, the system is working at that temperature level.

Estimations were made for some cases: test 1.2, 1.3, 2.2, 2.3, 3.2 and 4.2 of *table I*. Values are presented in *table II*.

Curves of losses are shown on *figure 4* for case 1.2, 2.2, 3.2 and 4.2. An interesting heat transfer process can be noticed meanwhile. At the beginning, due to the difference of block and water heat content, heat transfer from blocks to water occurs until the temperature field becomes uniform. It can be observed by the increase of the water temperature or its heat content.

In the case of tests 3.2 and 4.2, characterised by higher heat dissipation rates, the overall average temperature of the box is considerably higher than in the other cases. The heat losses are more important. The reason for this is that heat is transferred from the box to the surroundings by both (natural) convection and by radiation; by the latter means, heat is proportional to temperature to the power 4.

These heat losses will serve for the boundary conditions in the numerical calculations. In fact to simplify the calculations, such configurations may be treated in 2D. Since it is difficult to estimate the distribution of heat losses through the six walls of the box, the overall heat losses are important for boundary conditions.

TABLE II
Boundary conditions.

Test	Mass flow rate ($m^3 \cdot h^{-1}$)	Heat dissipation rate (W)	Heat losses (W)	Input for computation (W)	Inlet temperature (°C)
1.2	0.2	1 573	320	1 253	35.7
1.3	0.3	1 573	300	1 253	34
2.2	0.2	3 400	400	3 000	47.1
2.3	0.3	3 400	400	3 000	51.4
3.2	0.2	5 105	1 100	4 005	51.9
4.2	0.2	6 968	1 200	5 768	63.2

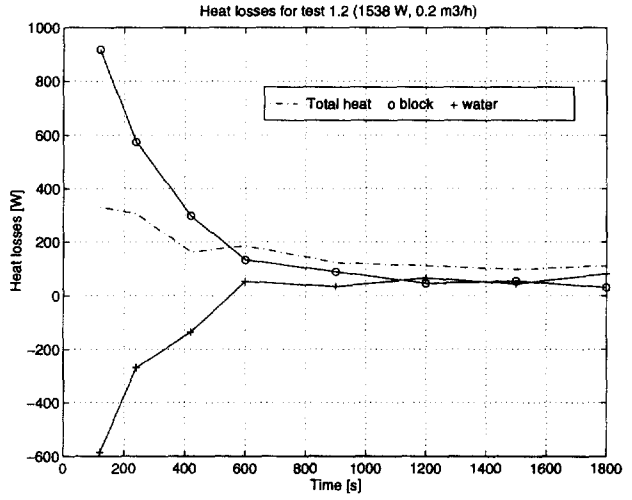

a

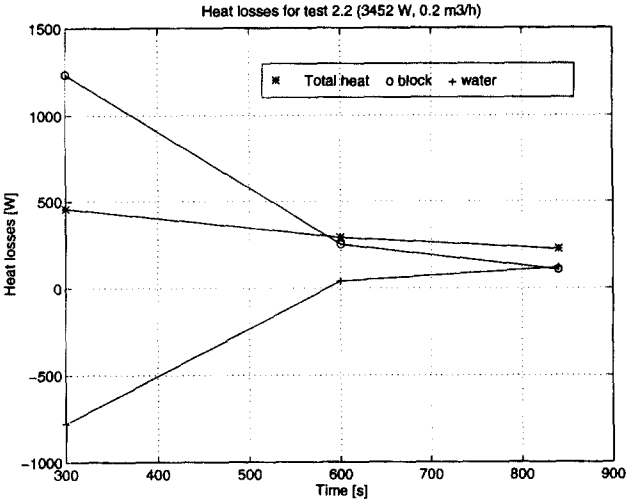

b

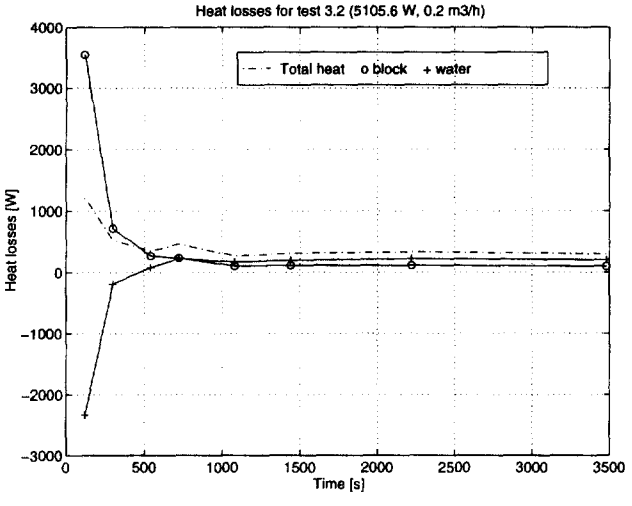

c

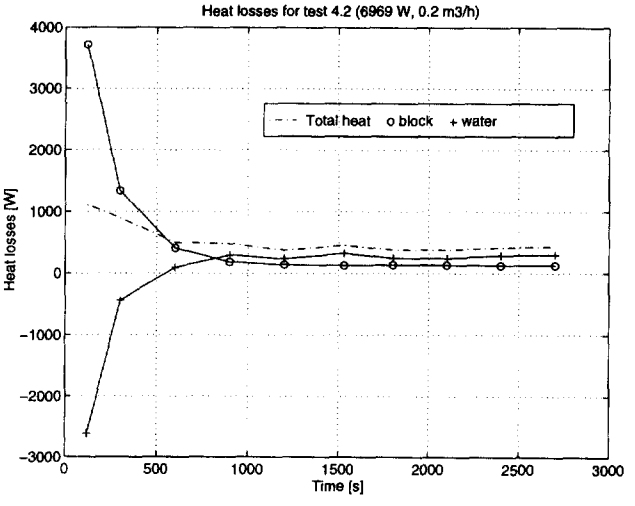

d

Figure 4. **a**. Heat losses test 1.2 ($Q = 1\,538$ W, 0.2 $m^3 \cdot h^{-1}$). **b**. Heat losses test 2.2 ($Q = 3\,452$ W, 0.2 $m^3 \cdot h^{-1}$). **c**. Heat losses test 3.2 ($Q = 5\,105.6$ W, 0.2 $m^3 \cdot h^{-1}$). **d**. Heat losses test 4.2 ($Q = 6\,969$ W, 0.2 $m^3 \cdot h^{-1}$).

2.4 Steady state temperature measurement

To get different measuring points, the horizontal thermocouples 1 to 6 in *figure 2* were set at three to four different positions to get the temperature in the first vertical channel, in the middle of the horizontal channels and in the central vertical channel. This is shown in *figure 5*. This *figure* gives a part of the temperature field in the fluid. Thermocouple 8 was set at four different positions in the central vertical channel. With thermocouple 9, surface temperature of blocks 7 and 8 were measured at the middle of their height. In addition, the fixed thermocouples set in the block give the temperature field in the blocks. We obtain thus a mesh of 11×19 for the temperature field. To get reliable values for each measurement, three values were noted for each location at three consecutive points of time at short intervals of one minute. The average was then used. These values will be compared with forthcoming numerical values. Corresponding values will be presented in § 3.4.2 together with the calculated temperature field. They are the numbers written on the *figure* and they correspond to the locations of thermocouples shown in *figure 5*.

2.5. Velocity measurement

Concerning measurements performed for velocity field, as specified above, the LDV technique is used.

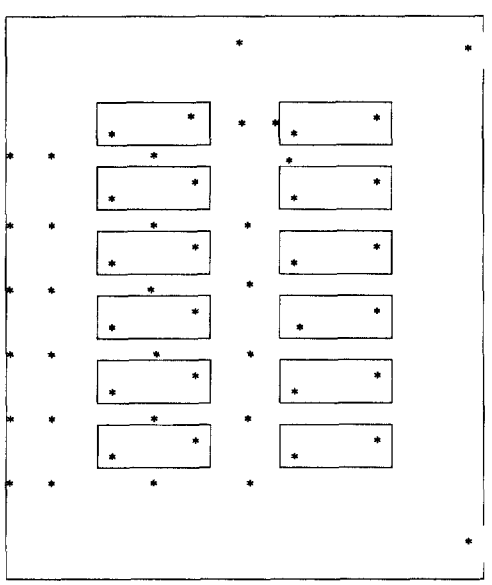

Figure 5. Locations of temperature measurement points (character*).

The characteristics of the beam were as follow:

- resolution [mm]: 0.1609, 0.1605, 2.2233 in respectively the x, y and z direction. The z direction is the direction perpendicular to the front wall, in accordance with the accuracy of the positioning system;
- wavelength [nm]: 514.5
- lens focal length [mm]: 310
- beam separation [mm]: 59.99.

The difficulties faced in this case were:

- the lack of significant number of particles supposed to run in the fluid in order to be captured by the laser beams;
- the reflection of the laser beam light due to the box configuration and the front wall of the box in Plexiglas, and also to some scratches due to its use;
- the dirtiness of the front wall in Plexiglas, avoiding thus a good penetration of the beam.

The particles (aluminium powder) were inserted from the pressure relief vessel on top of the set-up. After a certain while, they were all trapped in the radiator and in some other parts in the entire loop.

To avoid reflection, the laser beam was set in an oblique position at an angle $\alpha = 10°$ with respect to the front wall of the set-up. A correction factor cosine α according to *figure 6* is used to get right components. Concerning the dirtiness of the front wall, after a certain time (days to weeks) when the sensibility of the measurement decreased due to dust, the water was renewed and a sponge hung on the wall was regularly used to clean it.

The accuracy for a measurement point is estimated by means of the corresponding Root Mean Square (RMS), according to the following formula (Bentley [3]):

$$\text{error} = \frac{3\,RMS}{\sqrt{\text{number of validated samples}}} \qquad (3)$$

The expected 1 000 validated samples were reached for all the points at less than 4 mm from the wall,

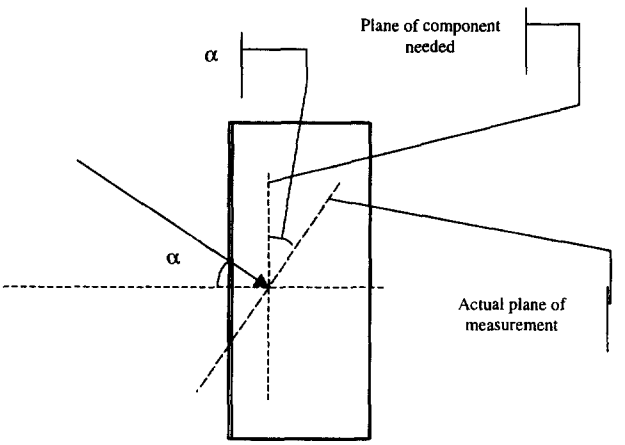

Figure 6. Deviation of the laser beam to avoid reflection.

since the flow regime is mixed convection. At greater distances, fewer particles could be captured and the errors for the given points were more important, and so the measured value could not validate the numerical calculation.

Moreover, it was quite impossible to measure a velocity of magnitude smaller than 0.001 $m \cdot s^{-1}$ by means of the laser setting available; it has been possible to measure only velocities of greater magnitude i.e. those close to the heated walls. In fact, due to the mass flow rate and heat dissipation rate ranges, the flow regime is mixed convection with a dominating influence, the buoyancy forces. The greatest velocity values are thus adjacent to the walls. And as a matter of fact a presentation of the complete domain has not been possible for the measured values. Since the work deals with comparison of calculated and measured values (performed at defined locations in the domain), the values at the common locations are compared and presented. Moreover they are the greatest and errors on them are more significant.

The numerical calculations give of course detailed values for the whole field.

3. NUMERICAL CALCULATION

The geometrical model used to simulate numerically the flow is presented in *figure 7* with its sub-regions and the corresponding meshes. A part of the loop of *figure 1b* is considered. The simulation is two-dimensional and the regime is laminar. For each region in the y direction the grids are distributed symmetrically with an exponential law of 7 to have a good refinement near the walls. Such distribution is applied at the fluid-solid interface to face the drastic change of properties. In the z-direction, the same distribution is used except for the block region where a smaller exponent (equal to 2) is used.

3.1. Three dimensional effects

The frontal width (third dimension, i.e. perpendicular to the front wall of the set-up) of the transformer box is 0.2 m. The maximum mass flow rate considered for the present experiment is 0.3 $m^3 \cdot h^{-1}$. This value has been chosen to avoid the influence of the horizontal orientation of the inlet flow on the main flow. With such value, the mean velocity in the box is: $\dot{v} = A\,v$.

$$v = \frac{\dot{v}}{A} = \frac{\dfrac{0.3}{3\,600}}{19 \times 10 \times 10^{-4}} = 2 \cdot 10^{-3}\ m \cdot s^{-1}$$

A stands for the cross section area of the transformer available for the fluid to flow up-stream. Viewed from the profile (considering the third dimension), the flow in each vertical channel may be viewed as a flow with mean velocity of $2 \cdot 10^{-3}$ $m \cdot s^{-1}$ between two parallel plates placed at 0.2 m from each other. It is obvious that at the middle of this 'duct' or even in a certain width close to the channel width, walls do not influence the velocity profile.

The lens used to measure velocity has a focal length of 60 mm and allowed measuring at different locations in the third dimension. On the frontal line values of velocity proved to remain the same on a range from 2 cm from the front wall up to 14 cm. Further, no measurements seemed to occur (due to the sensitivity of the Laser system).

It is at the bottom of the box, below the two columns of blocks that the flow may present a 3-dimensional feature, since the fluid streams from a small area (inlet) to the bottom space, which is greater in size. These effects vanish up stream and may be neglected. The same argument prevails in the space above.

3.2. Governing equations

The Navier–Stokes equations are used to describe the heat transfer and the laminar fluid flow. It is a conjugated heat transfer problem since heat is transferred both by convection and conduction within the box. At the interface solid–fluid, the harmonic average k_i of k_{bl} and k_f is used since the two conductivities have two values drastically different. k_i is defined below.

$$k_i = \frac{k_{bl}\, k_f\, (y_p + y_s)}{k_{bl}\, y_p + k_f\, y_s} \tag{4}$$

y_p and y_s are respectively the distance between the centre of the cell in the fluid region at the interface fluid–solid and its interface with the adjacent solid cell, and the distance between the centre of the cell in the solid region at the interface fluid–solid and its interface with the adjacent fluid cell.

A Heavyside function equal to 1 in the regions where the heat sources are active, i.e. in the block region, and equal to 0 in the other part of the domain is used to take into consideration correctly the distribution of heat dissipation rate.

The buoyancy forces are taken into account in the w-momentum equation, since for the ranges of mass flow and heat dissipation rates, mixed convection is present with even the dominating effect of buoyancy forces.

Numerical calculations are performed corresponding to some experiment conditions to validate them. The above experiments provide the boundary conditions for the numerical simulations. The numerical code Phoenics is used.

The velocity boundary conditions are:

- inlet through the entrance free flow area at the bottom:

at $z = 0 : v = v_{in}$ uniform inlet velocity calculated from mass flow rates of *table II*;

– outlet at the top right side:

at $z = z_f$, $\frac{\partial}{\partial z}$ of p, v, w and $T = 0$.

No slip at the interface fluid-wall.

The fluid (water) properties are (Fundamentals [4]).

$$\rho = -0.1\,T + 1\,000.4 \quad (5)$$

$$C_p = -2.3\,T + 4\,233.7 \quad (6)$$

$$\nu = 1.07{\cdot}10^{-10}\,T^2 - 2.115{\cdot}10^{-8}\,T + 0.1357{\cdot}10^{-5} \quad (7)$$

$$k = 2.6{\cdot}10^{-3}\,T + 0.5513 \quad (8)$$

During the experiments, heat losses through the walls have been estimated. This estimation consists of the value of the heat losses through the whole wall. No indication is given about the distribution per wall or surface. Thus, to avoid the uncertainty in wall heat loss estimation for the numerical simulation, the heat dissipation rate considered for the numerical simulation, Q_{comp} is the net heat input, calculated as follow:

$$Q_{comp} = Q_{real} - Q_{loss} \quad (9)$$

Consequently, the boundary condition for the heat flux at the walls is: $\frac{\partial T}{\partial n} = 0$.

The inlet boundary conditions for temperature and velocity are mentioned in *Table II.*

The grid setting is shown in *figure 7.* This setting was chosen by intuition, guided by some experience but will be checked by comparison with the measured values. Thus no grid independence study is performed at this stage.

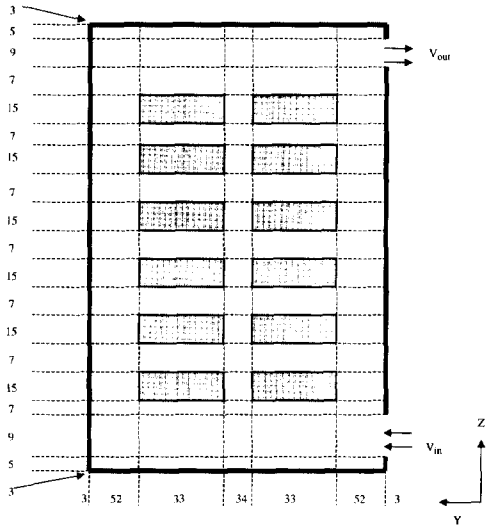

Figure 7. Computation domain and grid setting.

3.3. Numerical parameters

According to the policy statement on numerical accuracy, numerical parameters values and adjustments should be mentioned to estimate the uncertainty.

For temperature, false time relaxation was 10 at the beginning of the simulation and after calming down, it was raised to $1.0{\cdot}10^3$. For velocity components and pressure, the value of 0.4 seemed to fit. After a couple of sweeps, values were raised to about 0.8. These small values were necessary to ensure small changes in the calculated values from one iteration to the other. In fact, in buoyancy dominating flow, convergence is hard to reach. For density on the other hand, it is the linear relaxation that was applied. A value of 0.7 seemed convenient. This means of under relaxation i.e. linear relaxation is recommended for quantities that are not computed by means of differential equations [6].

An implicit formulation is used for the finite-domain equations. This means that in the discretisation formula for the given variable, the neighbouring calls' variables are those which prevail at the current time step. This is generally used, except if one needs computing economy.

The convergence criterion is based on the sum of the residuals of algebraic equations, which is set to:

$$\frac{\sum |R|}{R_{ref}} < 1 \cdot 10^{-3}$$

Also the successive changes of the solved for variables for the flow field are monitored. It is defined as the ratio of the difference between the variable value of the present iteration $\phi^t_{i,j}$ and the value of the previous iteration $\phi^{t-1}_{i,j}$, divided by the value of the present iteration. Thus convergence can be declared, for successive changes, as $1{\cdot}10^{-5}$:

$$\left| \frac{\phi^t_{i,j} - \phi^{t-1}_{i,j}}{\phi^t_{i,j}} \right| \sim 1 \cdot 10^{-5}$$

The number of sweeps rose to 3 500 to satisfy convergence. Under-relaxation also needed many adjustments to avoid divergence.

3.4. Results

3.4.1. Velocity field

An interesting velocity profile can be observed in *figure 8,* for test 2.2. A set of eight different tests has been performed for this investigation. Figures describing the temperature and velocity profiles are presented only for one test (test 2.2) to avoid great numbers of figures in this article (eight times more).

For clearness, only vectors close to the walls are presented and magnified. They are to be compared

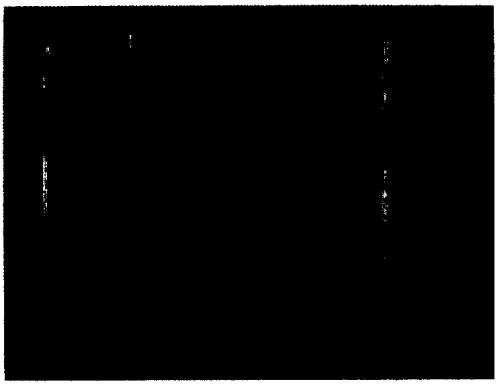

Figure 8. Profile of calculated velocity close to the walls for test 2.2 (for better view, vectors in horizontal channels are not presented).

with measured values. The whole field can thus not be presented. For the same reason the vectors in horizontal channels are not displayed. It can be noticed that the buoyancy forces are dominating the inertia forces.

For comparison, only the corresponding points of the measurement in the velocity field of the numerical calculations are extracted. The velocity field for test 2.2 is presented in *figures 9a* and *9b*. In *figure 9c*, a zoom of the region 0.2–0.27, 0.2–0.29 is presented for a clear view of the vector positions.

The different figures present the same profile. As mentioned above on some figures, the values presented are measured at some points and for the cases where buoyancy effects are significant, it is close to the wall that the velocities are more important and thus the accuracy in the measurement is higher. At some distance from the wall, due to the very small values of the velocity ($1.0 \cdot 10^{-4}$) less accuracy occur.

Tables III and *IV* represent the percent errors for the velocity field. The errors for the vertical velocity vectors are quite acceptable, being less than 15 % for most of the points. Since the main flow is vertical, the effect on the accuracy is less influenced by the horizontal components of the velocity. The differences between the measured and the calculated values can be on one hand, blamed on the reasons mentioned above for the temperature, and on the other hand, on the inaccuracy in the location of the laser beam due to the hysteresis of the material. Since the velocity boundary layer in the buoyancy case is thin, a small displacement of the beam gives another value that may be the half of the value just few millimetres distant.

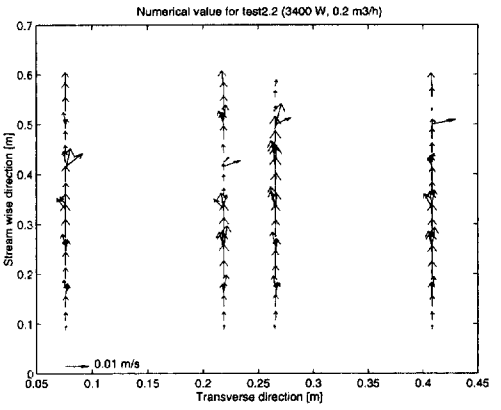

a

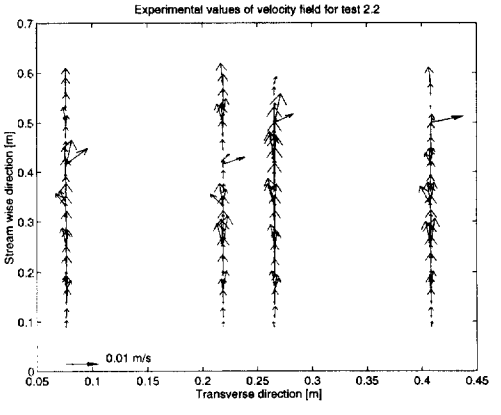

b

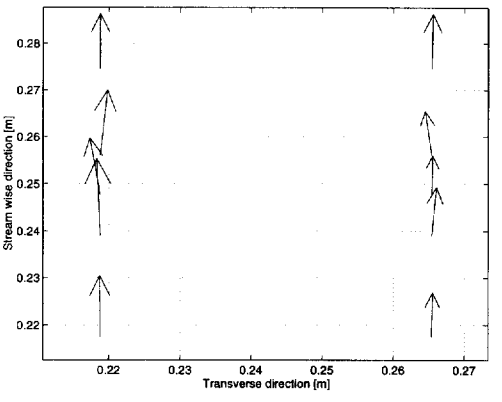

c

Figure 9. a. Calculated velocity field for test 2.2. b. Measured velocity field for test 2.2. c. Zoom of b, region (0.2–0.27, 0.2–0.29) (test 2.2).

3.4.2. Temperature field

Figure 10 shows the calculated temperature field for test 2.2. A comparison with the measured values corresponding to the locations presented on *figure 5* is made. *Table V* shows only the differences in the temperature larger than or equal to 2 K in absolute value.

Comparison of temperature fields gives some differences shown in *table V*. Especially in the horizontal channels big differences occur. They are regions requiring much caution in treatment. On the other hand,

TABLE III
Difference between calculated and measured vertical velocities.

Errors on vertical velocity for test 2.2.

Points	Errors (%)	Points	Errors (%)	Points	Errors (%)	Points	Errors (%)
1	23.3	30	10.9	59	6.8	88	9.3
2	12.3	31	12	60	5.7	89	5
3	9.7	32	4.7	61	8.8	90	2.9
4	4	33	8.5	62	5.4	91	2.4
5	16.9	34	11.5	63	7.1	92	6.9
6	5.3	35	14.8	64	6.3	93	3.9
7	37.7	36	11.2	65	2.5	94	2.5
8	7.9	37	10.1	66	6.5	95	1.6
9	6.8	38	5.1	67	3.4	96	3.4
10	9.4	39	4	68	8.5	97	1.7
11	4.3	40	1	69	3	98	2.9
12	4.7	41	10.9	70	0.6	99	1.8
13	5.4	42	5	71	2.3	100	2.8
14	2.2	43	1.6	72	2.2	101	4.5
15	10.2	44	8.9	73	3.8	102	1.5
16	6.9	45	4.6	74	1.9	103	1.5
17	4.3	46	4.8	75	1	104	4.3
18	–	47	6.2	76	3.5	105	1.6
19	5.2	48	8.9	77	2.1	106	2.8
20	9.6	49	12.5	78	1	107	5.2
21	15.6	50	14.3	79	1.5	108	1.3
22	9.2	51	1.3	80	1.4	109	1.1
23	4.8	52	7	81	1.4	110	1.9
24	10.5	53	3.2	82	2.1	111	1.1
25	11.1	54	1.6	83	4.7	112	4.2
26	7.8	55	4.2	84	15.4	113	20
27	15.2	56	2.1	85	8.3	114	10.3
28	10.5	57	2.1	86	7.6	115	10.9
29	15	58	1.3	87	11.9	116	6.9

TABLE IV
Difference between calculated and measured horizontal velocities.

Errors on horizontal velocity for test 2.2.

Points	Errors (%)	Points	Errors (%)	Points	Errors (%)	Points	Errors (%)
1	33.3	30	–	59	20	88	50
2	200	31	100	60	50	89	–
3	400	32	100	61	100	90	–
4	55.6	33	12.5	62	11.1	91	16.7
5	16.7	34	33.3	63	11.8	92	–
6	42.9	35	16.7	64	11.1	93	12.5
7	200	36	100	65	100	94	–
8	100	37	–	66	100	95	–
9	25	38	12.5	67	12.5	96	16.7
10	0	39	–	68	33.3	97	–
11	15.4	40	–	69	14.3	98	18.2
12	200	41	–	70	50	99	–
13	–	42	–	71	100	100	–
14	–	43	8.3	72	16.7	101	12.5
15	16.2	44	4.7	73	5	102	5.9
16	13.6	45	18.2	74	4.8	103	10
17	50	46	–	75	33.3	104	–
18	100	47	–	76	100	105	–
19	9.5	48	50	77	20	106	14.3
20	4.2	49	2.8	78	10	107	–
21	16.7	50	12.5	79	11.8	108	–
22	–	51	33.3	80	100	109	–
23	–	52	100	81	–	110	–
24	16.7	53	28.6	82	19.2	111	50
25	25	54	9.5	83	8.8	112	1
26	11.1	55	12.5	84	50	113	20
27	100	56	–	85	100	114	50
28	–	57	–	86	–	115	–
29	–	58	22.2	87	14.3	116	16.7

good agreement was noticed in the other regions. The energy balance was also respected for the whole domain, i.e.

$$Q_{\text{input}} = (T_{\text{out}} - T_{\text{in}}) \times \text{mass flow rate} \times \text{mean specific heat of water} \quad (10)$$

To face the inaccuracies of temperature field in these critical regions, the grid setting must be locally readjusted. In fact, in laminar flow contrary to turbulent flow, the grid setting is responsible for the wall friction at the interface fluid-solid [5, 6]. The main reason for treating them differently in relation to the other areas, is the type of flow within these regions. The flow is cross-flow oriented, the magnitude of the velocity is very small, some stagnant flow may also be noticed as well as vortices.

Also at the junction, flow separation gives some degree of complexity to the region. Thus a new grid refinement was set in those regions; the number is doubled. The mesh is then in the z-direction: 3, 5, 17, 13, 15, 13, 15, 13, 15, 13, 15, 13, 15, 13, 17, 5, and 3.

The underlined values are those modified with respect to the former setting.

The number of cells is just increased intuitively to check whether the calculated temperatures match the measured ones. Nevertheless from some library cases of conjugate heat transfer in the computor code package [6], such grid settings were used with less refinement. Since calculated temperatures and velocities can be directly compared with measured values; it is no longer necessary to make a grid-independence study.

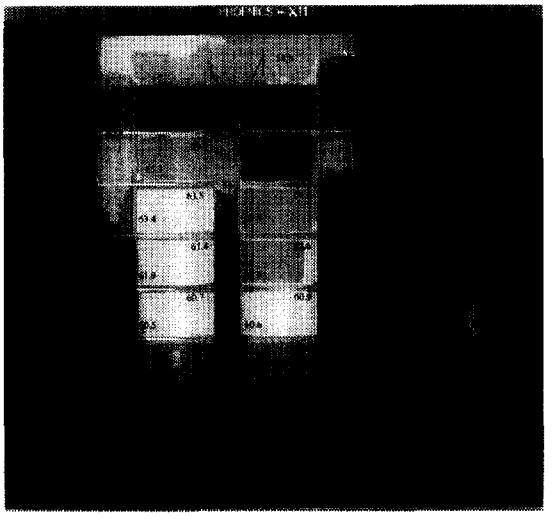

Figure 10. Comparison between measured and calculated temperature for test 2.2.

TABLE V
Differences between measured and calculated temperatures.

Location	Test 1.2	Test 1.3	Test 2.2	Test 2.3	Test 3.2	Test 4.2
13			−3			+2
16		+4.5	+6	−4	−4.5	−6
19	−4	+2.2	−2	−11		
22	−4	−3	−9	−11	−5	
25	−4	−3.5	−7	−5	+2	
39			−3	−2		

With the new grid setting the improvement is obvious. In this case the differences (even less than 2 in the whole region) are shown. *Figure 11* compares the new calculated results with the measured ones. Comparison of measured and calculated values shows that a tight refinement of grid in the horizontal channel was necessary to get a good agreement. The differences were especially noticed in the horizontal channels between the blocks. For temperature. the greatest differences between the measured and the calculated values fell from about 9 degrees for the first mesh to some 3 degrees with the last grid refinement. *Table VI* shows these new differences.

For the velocity field no great difference was noticed between the first grid setting and the refined one. The dissipated energy may also be compared between the experimental results and the numerical calculations. Equation (10) is thus used to estimate the energy removed experimentally; the values obtained from this operation are compared with the input heat dissipation introduced for the numerical computation mentioned in *table II.*

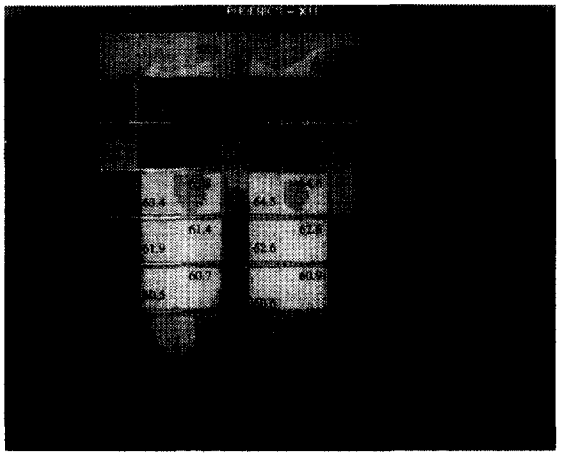

Figure 11. Temperature field due to the new grid refinement (measured values are numbers written on the figure).

TABLE VI
Differences between measured and calculated temperatures for the new grid refinement.

Location	Test 1.2	Test 2.2	Test 2.3	Test 3.2
11		−2		
13	+1	+1	+2	+2
14				+2
16	+2	+1		+1
17				+2
19	−3	−1	−2	−2
22		−3	−4	−4
25			−3	
39		−1	−3	
40	+1			+2
44	−1			−2
46	−1			−2
48	−1			

To calculate expression (10), equations (5) and (6) are used. The arithmetic average of inlet and outlet temperatures is used in the calculation. This is a good approximation because in view of the temperature profile of *figure 10*, the temperature evolution in function of the height is somewhat linear. *Table VII* presents the comparison of experimental and numerical values of heat removed by the fluid. The values agree to within 4 to 15 % of each other. That is acceptable. The validation method is similar to that used in [1].

4. CONCLUSION

An experimental set-up simulating the cross-section of a disc-type transformer has been designed for the validation of numerical calculations performed on similar configurations. The set-up is made of a box in

TABLE VII
Comparison of heat removed by the fluid from the experimental results and from the numerical calculations.

Test	$T_{outlet} - T_{inlet}$ (°C)	Mass flow rate ($kg \cdot s^{-1}$)	Heat removed from experimental values (W)	Heat removed from numerical calculations (W)	Error (%)
1.2	5.1	0.055	1 170.6	1 253	6.6
2.2	11.5	0.055	2 614.5	3 000	12.9
3.2	16.9	0.055	3 822.9	4 005	4.5
4.2	21.7	0.055	4 864.3	5 768	15

which two columns of six blocks are arranged in-line. Three heating elements are placed within each block to simulate the losses in the transformer windings. Temperature and velocity fields were measured by means of thermocouples and laser doppler velocimeter respectively. The instruments were well calibrated before conducting experiments. Measurements were performed with sufficient accuracy. Mass flow rate ranged between 0.1 and 0.3 $m^3 \cdot h^{-1}$ of water. This last value was considered as a maximum to avoid the effect of the horizontal orientation of the inlet (and outlet). Concerning the heat dissipation, values in the range between 1 500 and 7 000 W were used and combined with the mass flow rate value and gave a set of 8 different tests. Heat losses through walls were estimated and used to adjust the boundary conditions for numerical calculations. Numerical calculations were performed considering a two-dimensional flow around two columns of rectangular blocks. The cross-section of each block is idealised as a homogeneous section in copper. Comparison of measured and calculated values shows that a tight refinement of the grid in the horizontal channel was necessary to get a good agreement. The differences were especially apparent in the horizontal channels between the blocks. For temperature, the greatest differences between the measured and the calculated values fell from about 9 degrees for the first mesh to some 3 degrees using the last grid refinement. Concerning the velocity field, errors were for most of the measured points less than 15 %. This concerns the component in the main direction of the flow (vertical). Less accuracy were noticed for the horizontal components but due to their small magnitude (ten times less), the net accuracy of the CFD model can be considered as acceptable.

Reliability of CFD

The first grid setting has shown some differences between measured and calculated temperature values, especially in horizontal channels. There are regions where flow velocity is very small ($1.0 \cdot 10^{-4}$ $m \cdot s^{-1}$). A better refinement of grids in these regions improved the convergence between calculated and measured values. Indeed with CFD, temperature distribution is more detailed and overheating risk may be estimated, but it is not within the scope of the present study.

Information for other studies

This study might be applied in any configuration featuring an array of rectangular blocks arranged in-line. In such configuration, tight refinement must be set with logarithmic distribution allowing small cells at the interfaces. Moreover in regions with smaller velocity magnitude and dispersed (disturbed) velocity vectors, a tighter refinement should be set. In the present case a refinement of 13 cells in the horizontal channels of $14 \cdot 10^{-3}$ m width distributed logarithmically with a power 7, gave good results. The smallest cell sizes can thus be estimated. For the central channel the refinement is: 34 cells (in the cross-stream direction) distributed logarithmically with the same exponent 7. The central channel has a width of 5 cm. In this case the grid distribution at the interface cover the velocity boundary layer.

REFERENCES

[1] Yamaguchi M., Kumasaka T., Inui Y., Ono S., The flow rate in self-cooled transformer, IEEE T. Power Syst. 100 (3) (1981).

[2] Nakadate M., Toda K., Sato K., Biswas D., Nakagawa C., Yanari T., Gas cooling performance in disc winding of large-capacity gas-insulated transformer, IEEE T. Power Delivery 11 (2) (1996).

[3] Bentley John P., Principles of measurements systems, 2nd edition, John Wiley & Sons Inc., New York, 1988.

[4] Fundamentals, ASHRAE Handbook, 1989.

[5] Patankar Suhas V., Numerical heat transfer and fluid flow, Mc Graw-Hill Book Company, 1980.

[6] Phoenics Users Support, CHAM London, Correspondence 1995, Manuals.